

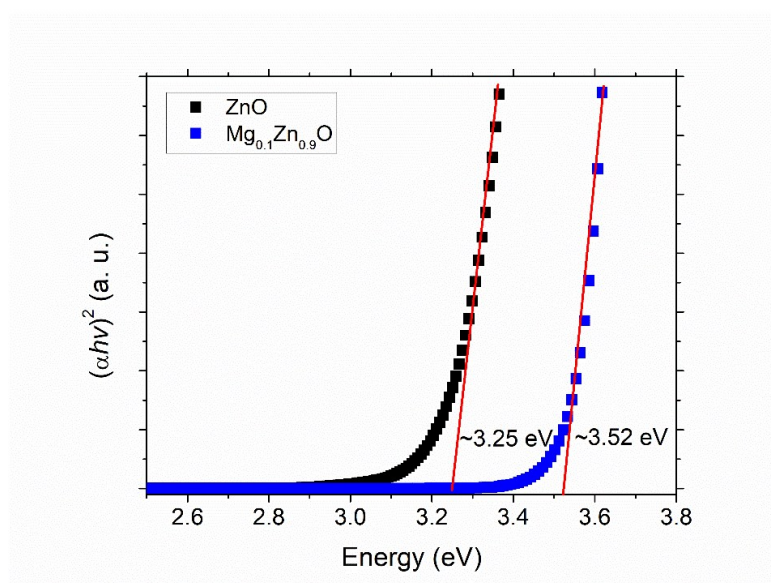
Supporting Information

Radial multi-quantum well ZnO nanorod array for nanoscale ultraviolet light-emitting diode

Jang-Won Kang, Byeong-Hyeok Kim, Hui Song, Yong-Ryun Jo, Sang-Hyun Hong, Gun Young Jung, Bong-Joong Kim, Seong-Ju Park*, and Chang-Hee Cho*

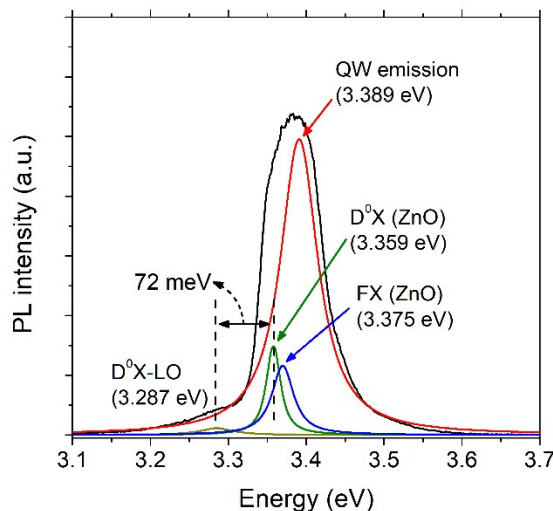
E-mail: sjpark@gist.ac.kr (S.J.P) or chcho@dgist.ac.kr (C.H.C)

Figure S1: Optical bandgap of MgZnO and ZnO layers for multiple quantum wells.



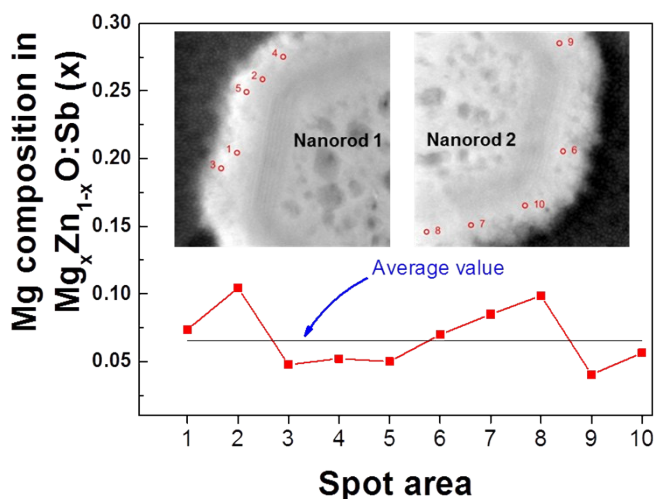
The optical bandgap of MgZnO and ZnO layers was estimated from the absorption spectra of the individual layers. The Mg composition of 10% in MgZnO layer was determined by the measured optical bandgap.¹

Figure S2: PL spectrum for near band edge emission at 10 K.



The emission peak was resolved by the deconvolution fitting of the broad spectrum, showing the QW emission at 3.389 eV, the free exciton emission (FX) at 3.375 eV, and the donor bound exciton emission (D⁰X) at 3.359 eV.² The peaks related with bulk ZnO such as the FX and D⁰X are most likely due to the bulk ZnO substrate. Importantly, the most intense peak at 3.389 eV, which is not matched with the ZnO related emission peaks, was assigned to the emission from MQWs.

Figure S3: Composition of Mg in MgZnO:Sb measured by EDS analysis at ten locations.



The band-gap energy of the *p*-type shell should be larger than the energy of light emitted from the MgZnO/ZnO MQWs because the light can be absorbed by the *p*-type MgZnO:Sb shell. Therefore, the incorporation of Mg in MgZnO:Sb is important because the band-gap of MgZnO:Sb is increased with Mg composition. To determine the Mg composition in

MgZnO:Sb, we measured the composition of Mg by EDS analysis of ten locations. The average Mg composition measured at ten different locations on two nanorods was 7%.

Figure S4: (a) Schematic illustration of the fabrication of the LED containing a core-multishell MgZnO:Sb/MQW/ZnO nanorod array. SEM images of (b) nanorods coated with SOG and (c) Ni/Au layer deposited on the exposed surface of nanorods with SOG.

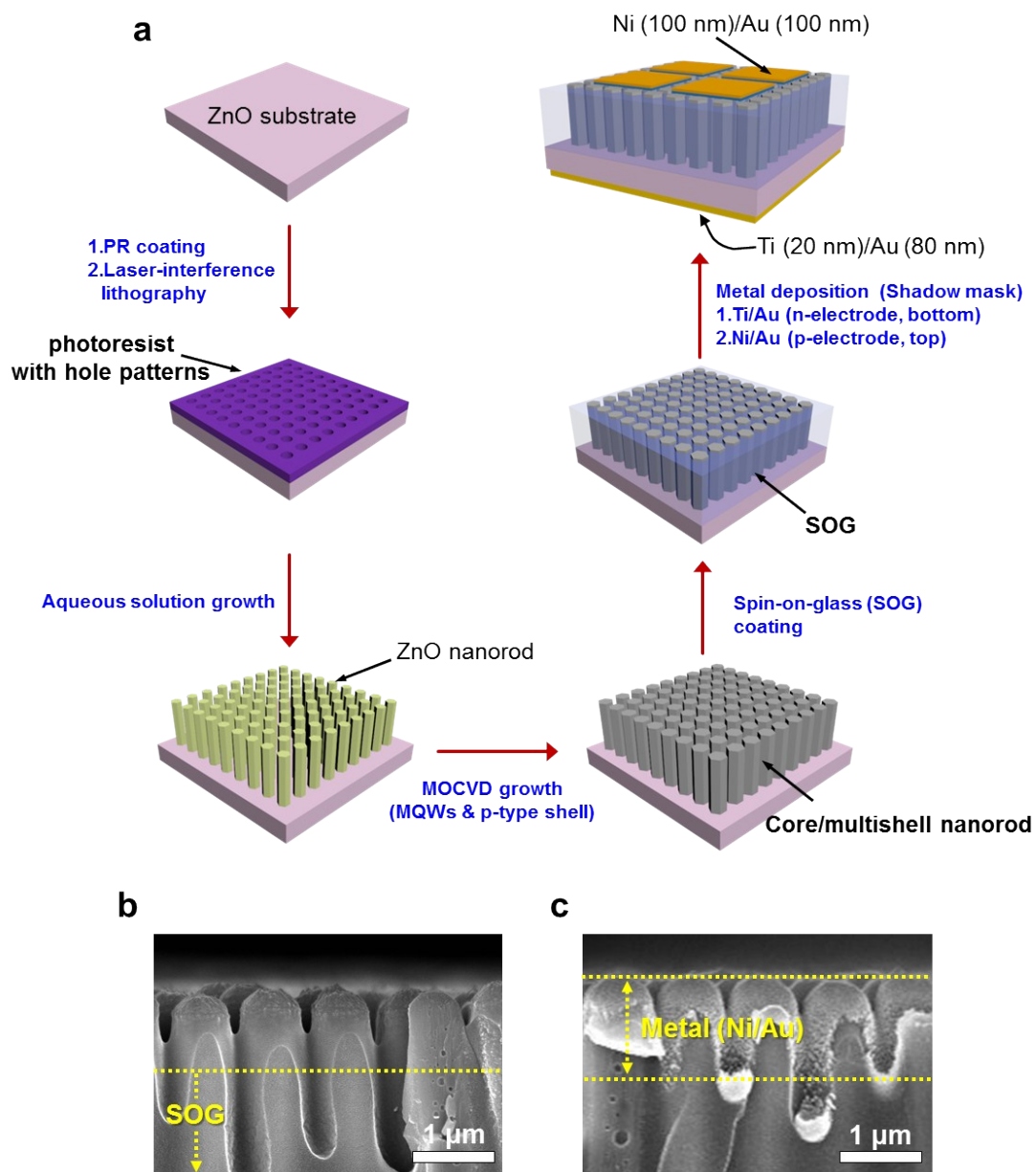


Fig. S4a presents a schematic illustration of the fabrication of a LED containing core-multishell MgZnO:Sb/MQW/ZnO nanorod array. A regularly patterned ZnO nanorod arrays was fabricated by growing ZnO nanorods on a hole-patterned PR layer. The multishell layers

of MgZnO:Sb and MGZnO/ZnO MQWs were grown on the ZnO nanorod array by MOCVD. Spin-on glass (SOG) was spin-coated onto the arrays as a supporting layer. To expose an upper area of the side walls as well as the top of nanorods for metal contact, the SOG spin-coating process was optimized as shown in the SEM image of Fig. S4b. The SOG was spin-coated on the nanorod array at a rate of 1000 rpm for 1 min. The top contact of Ni/Au (100/100 nm) was deposited on the *p*-type MgZnO:Sb shell by e-beam evaporation. Fig. S4c shows that the Ni/Au contact formed well on the nanorod and SOG. Ti/Au (20/80 nm) was used as a bottom contact to the ZnO substrate.

Figure S5: Dependence of the carrier concentration of MgZnO:Sb on annealing temperature.

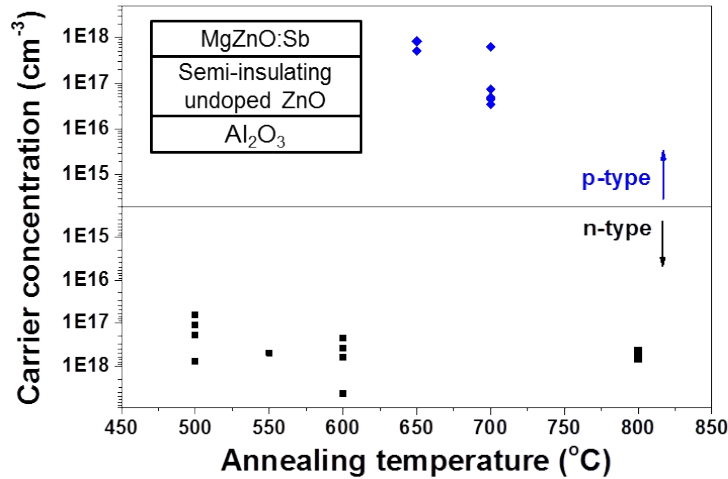
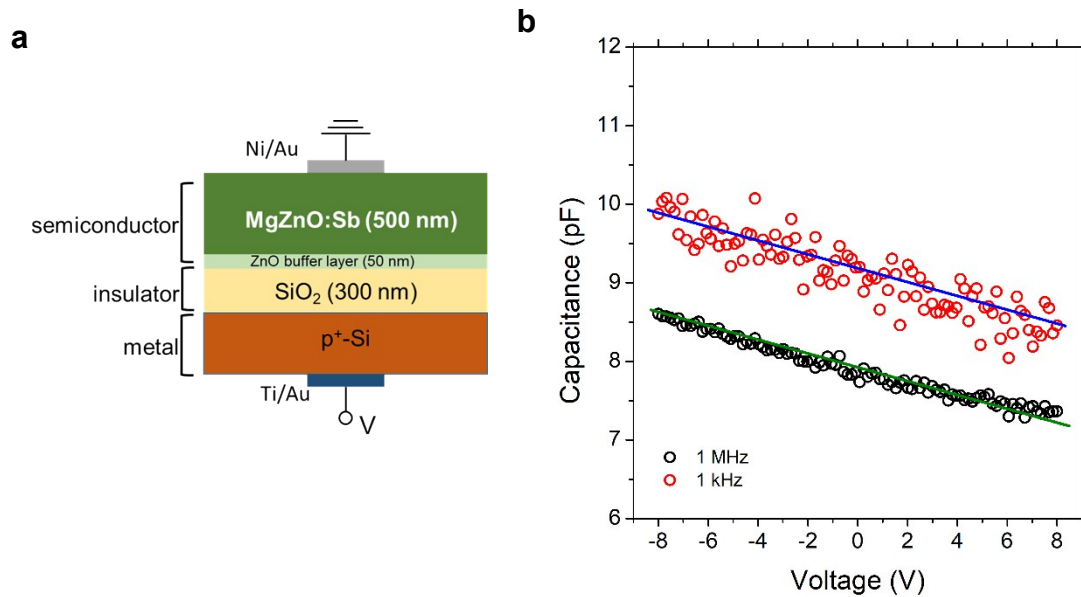


Table S1. Electrical properties of MgZnO:Sb annealed at 700 °C. Electrical properties were determined by Hall measurements in the van der Pauw configuration at room temperature.

Sample	Mobility (cm ² /V·s)	Concentration (cm ⁻³)	Type
1	4.12	4.43×10 ¹⁶	p
2	2.33	7.44×10 ¹⁶	p
3	0.269	6.30×10 ¹⁷	p
4	3.36	4.94×10 ¹⁶	p

The conductivity of the MgZnO:Sb shell could be determined by Hall measurements of a MgZnO:Sb layer grown on an un-doped ZnO template because the MgZnO:Sb shell was uniformly grown on the ZnO nanorod core under the same growth conditions. To obtain a MgZnO:Sb shell with *p*-type conductivity, the MgZnO:Sb shell grown by MOCVD was post-annealed at temperature from 500 to 800 °C. Post-annealing was conducted by a rapid thermal annealing process under N₂ ambient condition for 1 min. MgZnO:Sb grown at 600 °C exhibited semi-insulating electrical properties and was converted to *p*-type MgZnO:Sb after rapid thermal annealing.³ As shown in Fig. S5, *p*-type MgZnO:Sb could be obtained at annealing temperatures from 650 to 700 °C. The *p*-type conductivity of MgZnO:Sb was reproducibly obtained from samples annealed at 700 °C. The electrical properties of four samples annealed at 700 °C are presented in Table S1.

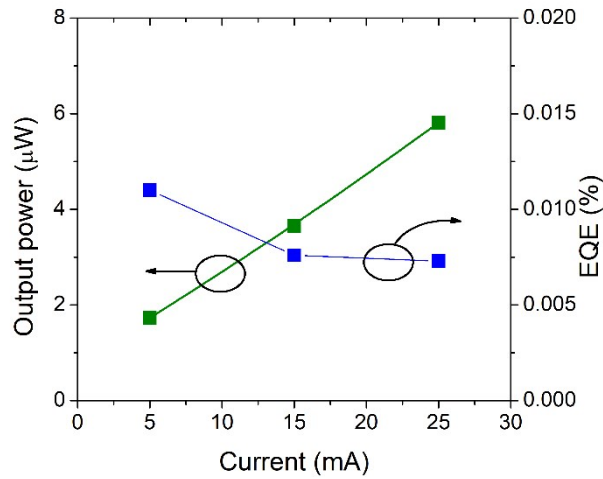
Figure S6: Capacitance-voltage (*C-V*) characteristics of MgZnO:Sb layer.



The *C-V* characteristics of MgZnO:Sb layer have been performed by fabricating the metal-insulator-semiconductor (MIS)-type diode of MgZnO:Sb/SiO₂/p⁺-Si (Fig. S6a). To prevent the deterioration of the crystal quality, the ZnO thin buffer layer (~50 nm) was grown on SiO₂ layer by RF-sputtering deposition. When a negative voltage is applied to the p⁺-Si, the MIS capacitance is maximized because the negative bias accumulates holes at the MgZnO:Sb/insulator interface, and the capacitance gradually decreases as the bias increases. Therefore, the *C-V* curve shows a negative slope for a *p*-type semiconductor at high frequency.

As shown in Fig. S6b, the C - V curve of MgZnO:Sb layer shows a negative slope, indicating the characteristic of a p -type semiconductor at the depletion region.^{4,5} Thus, we could confirm the p -type conductivity of MgZnO:Sb layer.

Figure S7: Optical power measurement and external quantum efficiency of MgZnO:Sb/MQW/ZnO LEDs.



The optical output power was measured for the MgZnO:Sb/MQW/ZnO nanorod LEDs as a function of injection current, as shown in Fig. S7. We have measured the EL intensity of the nanorod LED devices by using an optical-fiber coupled spectrometer. To estimate the output power from the measured EL intensity (counts), the corresponding power emitted was estimated by taking into account the sensitivity (~ 130 photons/count) of the detector at UV region and the energy per photon. Then, the actual total output power from the device was calculated by taking into account the solid angle for the free space coupling into the optical fiber with the diameter of 1 mm at the fiber-to-sample distance of 20 mm.

From the measured optical output power, the external quantum efficiency (η) was estimated by using the following equation,⁶

$$\eta = \frac{P/(h\nu)}{I/e}$$

where P is the optical output power, $h\nu$ is the photon energy, and I is the injection current. In addition, the luminous efficacy under a forward bias was estimated to be 1.37×10^{-1} lm/W by using the optical power and photometric eye sensitivity function provided in Ref. [6].

Reference

- [1] K. Koike, K.Hama, I. Nakashima, G.Y. Takada, K. I. Ogata, S. Sasa, M. Inoue, and M. Yano, *J. Cryst. Growth*, 2005, **278**, 288.
- [2] K. Wu, H. He, Y. Lu, J. Huang and Z. Ye, *Nanoscale*, 2012, **4**, 1701.
- [3] K.-K. Kim, H.-S. Kim, D.-K. Hwang, J.-H. Lim and S.-J. Park, *Appl. Phys. Lett.*, 2003, **83**, 63–65.
- [4] Y. W. Heo, Y. W. Kwon, Y. Li, S. J. Pearton and D. P. Norton, *Appl. Phys. Lett.*, 2004, **84**, 3474–3476.
- [5] Y. W. Heo, Y. W. Kwon, Y. Li, S. J. Pearton and D. P. Norton, *J. Electron. Mater.*, 2005, **34**, 409–415.
- [6] E. F. Schubert, in *Light-Emitting Diodes*, Cambridge University Press, New York, 2nd edn, 2006, pp. 85–86, 280–291.